Causal Evidence for Expression of Perceptual Expectations in Category-Selective Extrastriate Regions

Gandolfo, Marco; Downing, Paul

Current Biology

DOI:
10.1016/j.cub.2019.06.024

Published: 05/08/2019

Peer reviewed version

SUMMARY

Expectations about a visual event shape the way it is perceived [1–4]. For example, expectations induced by valid *cues* signalling aspects of a visual *target* can improve judgments about that target, relative to invalid cues [5,6]. Such expectation effects are thought to arise via pre-activation of a template in neural populations that represent the target [7,8] in early sensory areas [9] or in higher-level regions. For example, category cues ("face" or "house") modulate pre-target functional MRI (fMRI) activity in associated category-selective brain regions [10,11]. Further, a relationship is sometimes found between the strength of template activity, and success in perceptual tasks on the target [12–14]. However, causal evidence linking pre-target activity with expectation effects is lacking. Here we provide such evidence, using fMRI-guided online transcranial magnetic stimulation (TMS). In two experiments, human volunteers made binary judgments about images of either a body or a scene. Before each target image, a verbal cue validly or invalidly indicated a property of the image, thus creating perceptual expectations about it. To disrupt these expectations, we stimulated category selective visual brain regions (extrastriate body area, EBA; occipital place area, OPA) during the presentation of the cue. Stimulation ended before the target images appeared. We found a double dissociation: TMS to EBA during the cue period removed validity effects only in the body task, while stimulating OPA removed validity effects only in the scene task. Perceptual expectations are expressed by the selective activation of relevant populations within brain regions that encode the target.

Keywords: perceptual expectations; pre-stimulus brain activity; category-selective brain regions; transcranial magnetic stimulation; extrastriate body area; occipital place area

RESULTS AND DISCUSSION

We designed two visual tasks that demonstrate the effects of verbal cues on the efficiency of perceptual judgments, and that are aligned to suitable cortical targets for brain stimulation (Figure 1A). In a body perception task, valid verbal cues about the sex of a target body image ("m" or "f") improved the efficiency (mean RT / p(correct)) of judgments about the weight of the depicted person (heavy vs slim), relative to invalid cues, $t(24)=2.43$, $p=0.02$, $d=0.49$ (cf. [15]). In a scene perception task, valid verbal cues about the semantic category of a scene ("kitchen" or "garden") improved the efficiency of judgments about the target image's orientation (upright vs inverted; cf. [16]), relative to invalid cues, $t(24)=2.81$, $p=0.02$, $d=0.56$.

We then used online transcranial magnetic stimulation (TMS) in two experiments testing these two tasks, to establish that cue-driven neural activity in category-selective occipitotemporal regions is causally necessary for the expression of these validity effects. Neuroimaging studies have identified focal regions of occipitotemporal cortex that are selectively involved in body and scene perception. The activity of these regions relates to online visual representation of their preferred categories – for example, encoding body shape and posture [17,18] in the extrastriate body area (EBA), and describing scene geometry [19,20] in the occipital place area (OPA). Further, TMS studies have demonstrated a category-selective causal role for these regions in visual detection and discrimination tasks [21–26].

Using fMRI-guided TMS applied online during cue presentation (and ending before the target image appeared; Figure 1B; see also Table S1) we found that expectations in the body and scene tasks were selectively instantiated by activity in EBA and OPA respectively. In the first TMS study (N=21), a significant validity effect was found in the body perception task when TMS was applied to OPA ($t=2.14$, $p=0.045$, $d = 0.47$) but not to EBA ($t=-1.47$, $p=0.16$, $d = -0.32$; Site x Validity, $F(1,20)=5.3$, $p =0.032$, $\eta_p^2=0.21$). In the second study (pre-registered; N=21), an effect of cue validity was found in the scene task when TMS was applied to EBA ($t=2.70$, $p=0.013$, $d = 0.59$) but not to OPA ($t=0.57$, $p=0.57$, $d = 0.12$; Site x Validity, $F(1,20)=6.1$, $p=0.023$, $\eta_p^2=0.23$). Direct comparison of the two studies shows that the influence of cues on efficiency was disrupted in a task- and region-specific fashion (interaction of stimulation Site x Task x Validity in a mixed-design ANOVA, $F(1,40) = 11.34$, $p = 0.00017$, $\eta_p^2=0.22$). Collapsing over the two studies shows that when TMS was applied to the task-relevant regions (EBA for bodies, OPA for scenes), cue validity effects were on average eliminated (M = -1 ms, $t=-0.15$, $p=0.87$, $d = -0.02$) while they remained significant when TMS was applied to the task-irrelevant regions (EBA for scenes, OPA for bodies) (M = 26 ms, $t=3.33$, $p=0.0018$, $d = 0.51$) (Figure 2; see also Figure S1 and Table S2). Pre-target activity in category-selective regions is causally necessary to express the perceptual expectations generated by verbal cues.

We speculate that the expectancy effects revealed (and disrupted) here relate to domain-specific aspects of the structure of body and scene encoding in EBA and OPA respectively. For example, sex reflects a core division within visual body representations, due to its relevance over evolutionary and lifetime scales [27,28]. In turn, the representation of each sex can be characterised by distinct mental "spaces" that capture the relationships between

body shape and weight [29]. On this view, expectations in the body task are reflected in the selection of subsets of the spaces describing likely body shapes of the cued sex. This hypothetical selection process can be construed as a form of internal attention [30] or as a form of neural sharpening, as described in previous studies of expectancy effects in vision and action [31,32].

Turning to scenes, images of different environments differ in their visual properties, in the kinds and distribution of objects present, and in the boundaries and distances implied [33,34]. These considerations suggest two mechanisms by which expectancies ("kitchen" vs "garden") could facilitate judgments of scene orientation. First, scene gist enhances localisation and identification of expected objects [35–37], and such objects may in turn support a scene orientation judgment. Second, different environments differ in openness and in the number and nature of their boundaries [38]: while garden scenes tend to be open and contain fewer navigationally-relevant boundaries, indoor scenes such as kitchens are generally enclosed and more constrained. Such regularities may help to select the areas within a scene image that are diagnostic of its orientation. These proposals are consistent with evidence that OPA plays a role in encoding objects [39,40] and scene boundaries [20].

Our TMS findings are specific to the combination of stimulation site, task, and validity, ruling out several potential confounds. For example, these selective effects cannot be explained by distracting effects of peripheral muscle stimulation, by a general alerting effect of the cues, or by disruption of general linguistic processes related to reading those cues. Further, our study is better controlled than those that compare stimulation over an active site to sham stimulation, or to the vertex [41], because we stimulated two functionally comparable and adjacent (mean Euclidean distance between targeted peaks = 2.55 cm) sites. (Secondary planned ANCOVAs showed no evidence for a systematic inter-participant relationship between the distance between sites and the Stimulation Site x Validity interaction effects: body task: $p = 0.26$; scene task: $p = 0.28$).

Several lines of evidence suggest that the effects of stimulation were more likely related to processes triggered by the verbal cues than to spillover of TMS effects directly onto online visual perception of the targets. One line of evidence relates to the timing of relevant neural activity. Previous work showed that post-stimulus TMS over EBA is more effective than pre-stimulus TMS at interfering with performance on a person detection task [26]. Further, the earliest category-selective effects of TMS over EBA on a visual discrimination task are found over a narrow temporal window around 100-110 ms after stimulus onset, roughly 300 ms after the final pulse in our protocol [24]. While equivalent TMS data are not available for OPA, a recent magneto-encephalography study showed that a texture-independent representation of scene geometry likewise first emerges in this region at about 100 ms after stimulus onset [42]. Moreover, setting aside timing considerations, if TMS were directly impacting stimulus-driven perceptual processes, then we would expect overall performance to be impaired (collapsing over valid and invalid conditions) when task-relevant regions were stimulated, compared to task-irrelevant regions. In fact, in each experiment the non-significant trend was in the opposite direction (main effect of Stimulation Site: body task, EBA: 584 ms, OPA: 592 ms, $p=0.24$; scene task, EBA: 607, OPA: 577 ms, $p=0.08$). Alongside the significant Site x Task x Validity interaction, these findings strongly suggest that the main

impact of TMS in this study is on cue-related expectation processes rather than directly on image perception *per se*.

Other aspects of these tasks allow us to specify the expectation-related processes that they capture. First, in both tasks the cues were orthogonal to the task-relevant dimensions: they predicted which of two possible types the target would reflect, but not which response would be required. As such, the cue-related neural activity in EBA and OPA must have been related to forming expectations about the target itself, rather than about the decision or response required. Second, because the cues were in a different format than the targets, the effect of validity cannot be attributed to visual similarity between the cue and the target, and must instead have been at a more abstract level. Third, the targets in these tasks were presented in isolation and well above threshold. As such, the observed cueing effects were not related to filtering out distractors, or to consolidating awareness of ambiguous or near-threshold stimuli (cf. [43,44]). Finally, these findings are not attributable to state-dependent effects of TMS [45–47]: owing to the design counterbalancing, regional brain states at the time of brain stimulation were balanced, on average, with regard to the main validity manipulation.

Pre-stimulus brain activity in occipitotemporal regions is critical for the expression of perceptual expectations about those regions' preferred stimuli. This finding does not rule out additional causal contributions from other, domain general mechanisms. For example, selective attention may partly mediate the effects of an expectation on perception of the target. In the body task, for example, a sex cue may direct attention towards regions of the body that reliably distinguish heavy and slim people of that sex. As such, we see in these tasks an interplay between expectations generated by cues, and selection processes that facilitate turning those expectations into behavioural benefits. More broadly, forming perceptual expectations must also rely on flexible mechanisms that can interpret cues and relate them dynamically to current task goals. While the present findings do not speak to the neural basis of such mechanisms, a proposed hub-and-spoke network for controlled semantic cognition [48] appears to have the requisite components to link the verbal, visual, and semantic properties of people and places as tested here.

ACKNOWLEDGMENTS

We thank M. Peelen, C. Urgesi, K. Valyear, and the Bangor Imaging Group for valuable feedback and advice. L. Jacobs assisted with task development and data collection, and K. Darda with data collection. M.G. was funded by a PhD student grant from Bangor University.

AUTHOR CONTRIBUTIONS

M.G. and P.E.D. conceived and designed the experiments. Data collection was performed by M.G. M.G. and P.E.D. analyzed the data. The manuscript was written by P.E.D and M.G.

DECLARATION OF INTERESTS

The authors declare no competing interests.

FIGURE TITLES AND LEGENDS

Figure 1. Schematic illustration of task timeline and targeted brain regions. (A) Timeline of the body task (left) and the scene task (right). In each case, a written cue predicted, with 80% validity, a property of the target image that next appeared. Participants made a binary weight judgment on each body image (heavy vs slim) or a binary orientation judgment on each scene image (inverted vs upright). Display images not to scale. (B) fMRI-guided transcranial magnetic stimulation (TMS) was used to interrupt activity in body (left) and scene (right) selective occipitotemporal brain regions during the processing of the cues, and before the onset of the target images. Activation maps on gray-matter surfaces show representative localisation of extrastriate body area (EBA; left) and occipital place area (OPA; right). Point clouds on brain surface (centre) show, in MNI space, targeted peak locations for each participant x task combination (see also Table S1). Red: OPA, scene task; green: OPA, body task; blue: EBA, scene task; pink: EBA, body task.

Figure 2. Impact of TMS over extrastriate category-selective regions on cue-driven stimulus expectations. Mean efficiency scores across participants (RT / p(correct)) are plotted in relation to cue validity, separately for conditions in which TMS was applied to the task-irrelevant (left) and the task-relevant (right) brain regions. TMS during the cueing interval selectively eliminated effects of cue validity when applied to the task-relevant sites. Bars indicate mean values; error bars SE of the mean (including within- and between-participants variance); individual points reflect scores for each participant. See also Figure S1 and Table S2.

STAR METHODS

LEAD CONTACT AND MATERIALS AVAILABILITY

Further information and requests for resources and reagents should be directed to and will be fulfilled by the Lead Contact, Marco Gandolfo (m.gandolfo@bangor.ac.uk or marco2gandolfo@gmail.com). This study did not generate new unique reagents.

EXPERIMENTAL MODEL AND SUBJECT DETAILS

The procedures were approved by the Research Ethics Committee of Bangor University's School of Psychology. Participants were students at Bangor University and provided informed consent for their participation. They took part in return for course credit in a research methods module, or for a cash payment. No individual participant took part in more than one experiment.

Participants: Behaviour-only
Fifty-four participants took part in two experiments. Twenty-seven of these participated in the body perception task (4 males; mean age 20 $\pm$ 3) and twenty-seven in the scene perception task (5 males; mean age 21 $\pm$ 6). Two participants from each task were excluded because their mean accuracy or response times were 2.5 or more SDs above or below the group mean across conditions for that task. The final sample comprised 25 participants in each task.

Participants: TMS
Forty-seven participants took part in the TMS experiments. They were screened following the safety screening standard questionnaire for rTMS [49,50]. None of the participants reported any history of neurological, psychiatric or other major medical disorders. Twenty-three of these participants performed the body task (12 males; mean age: 24 $\pm$ 3 years) and twenty-four performed the scene task (6 males; mean age: 22 $\pm$ 5 years). One participant from the body perception task and one participant from the scene task were excluded because accuracy was 2.5 or more SDs below the group mean across conditions for that experiment. Three more participants (1 from the body perception task and 2 from the scene task) were excluded due to experimenter error or motion/discomfort during the stimulation. The final sample comprised 21 participants in each task. The sample size of the scene task was pre-registered to match the final sample of the body perception task together with the other experimental procedures (link: http://aspredicted.org/blind.php?x=xu95zn).

METHOD DETAILS

Imaging
Each participant in the TMS experiments first completed two to four runs of a four condition block-design functional localiser fMRI experiment in order to identify target sites for stimulation. The stimuli consisted of blocks of images of human bodies (without heads), unfamiliar faces, outdoor scenes, and chairs. Each condition was presented in four blocks of 18 sec in each run. These were interspersed with 5 fixation blocks of 16 sec duration,

resulting in a total of 21 blocks per run. In each block, 24 images (selected randomly from a full set of 40) were presented, each for 300 ms followed by a 450 ms blank interval. During each block, an image was presented twice in a row two times. Participants were instructed to detect these repetitions and press a key (1-back task).

Imaging data were acquired using a 3T Philips MRI scanner with a 32-channel SENSE phased-array head coil. Functional data (T2* weighted, gradient echo sequence; echo time, 35ms; flip angle, 90°) were acquired with the following scanning parameters: repetition time 2 seconds; 35 off-axial slices; voxel dimensions 3x3 mm; 3mm slice thickness; SENSE factor 2, phase encoding direction anterior-posterior. A high-resolution anatomical scan was also acquired (T1 weighted, 175 sagitally oriented slices; 1mm isotropic voxels; repetition time, 8.4 ms; echo time, 3.8ms; flip angle, 8°).

Functional MRI data were preprocessed and analysed using SPM12 [51]. The functional images were realigned and spatially smoothed (6-mm FWHM Gaussian kernel). The resulting images were entered into a subject-specific general linear model with four conditions of interest corresponding to the four categories of visual stimuli. Estimates of the BOLD response in each voxel and category were derived by a general linear model including the boxcar functions of stimulation that were convolved with a standard hemodynamic response function. All analyses were performed in participant-native coordinates; for reporting purposes, target sites were converted to standard MNI space.

In each participant individually, we localised right hemisphere body and scene selective regions by contrasting the response to human bodies with that to the remaining three conditions and the response to scenes with that to the remaining three conditions respectively. Each TMS target site (right hemisphere extrastriate body area [EBA]; right hemisphere occipital place area [OPA]) was individually identified by selecting the peak activation for that category in the relevant lateral occipito-temporal region based on previous findings [20,26]. The mean peak MNI coordinate (X, Y, Z, with SEs) was 48 (0.65), -71 (0.98), 2 (0.72) for right EBA and 34 (0.80), -79 (0.70), 20 (0.93) for right OPA (see also Table S1).

TMS stimulation

A Magstim Rapid^2 (Magstim; Whitland, UK) with a 70mm figure-eight coil was used for the TMS. Stimulation intensity was set at 120% of the resting motor threshold, defined as the minimal intensity of left motor cortex stimulation required to elicit a reliable MEP of at least 50 μV in the right hand's first dorsal interosseous muscle [52]. Online TMS was delivered at 10Hz (4 pulses, 1 pulse every 100ms for a total of 400 ms) with the handle pointing downwards approximately at 45° angle from the middle sagittal axis of the participants' head [25,53,54], adjusted to best project the pulse to the identified peak coordinate of each region and kept constant across stimulation site.

TMS targeting was managed with Brainsight 2.3.10 (Rogue Research Inc.), using individual structural and functional MRI images for each participant. The right EBA and right OPA were localized by overlaying individual activation maps from the localiser contrasts. The coil location was monitored online by the experimenter while participants performed the task, and was maintained within 1mm of the defined point. The screen displaying the

participants' task was out of view of the experimenter (MG), rendering him blind to condition on a trial-by-trial basis. To ensure temporal precision, the train of TMS pulses was triggered on each trial via a TTL pulse, initiated from a photosensor which detected a screen event (unseen by participants) that co-occurred with the cue onset on each trial.

Stimulus creation

Pictures of bodies were obtained through internet searches and were the same used in [15]. The pictures were grayscaled and cropped to exclude head and lower legs. Each body picture was presented at two different sizes (600 or 400 px height) to prevent the use of the proportion of pixels as a cue for weight judgments. Image width varied freely to maintain image ratio. Sixteen heavy and 16 slim male and female images were collected for a total of 64 images presented at two different sizes.

Pictures of scenes were obtained through internet searches. Pictures were greyscaled and resized to 450x450 px resolution. Twenty-five garden and 25 kitchen pictures were collected and rotated by 180° for a total of 100 pictures, 50 upright and 50 inverted.

Stimulus presentation

All stimuli were presented centrally on a 22 inch LCD monitor set at 1920x1080 resolution and a refresh rate of 60Hz. Image presentation was controlled by PsychToolbox [55] running on Octave 4 [56] for Linux OS (Version: Xubuntu 16.04).

Task Procedures

In the body task, participants were asked to judge on each trial the weight ("heavy" or "slim") of each body picture, which appeared after a verbal cue to its sex ("m" or "f"). In the scene task, participants were asked to judge the orientation of each scene ("upright" or "inverted") after a verbal cue to its content ("kitchen" or "garden"). In 80% of trials, the cue was *valid* – it matched the body or scene to be judged -- and in 20% of trials it was *invalid*. Judgments were made by pressing one of two keys ("f" or "j") on the keyboard. Participants were instructed to respond quickly and accurately.

Each trial was preceded by a central fixation with a random duration between 1.9 and 2.9 seconds. The written verbal cue was presented at the center of the screen for 500ms and followed by the body or scene target image, which appeared for 300 ms. Four TMS pulses at 10 Hz were applied, starting at the onset of the verbal cue and finishing 200ms before image onset. Participants performed 160 trials per stimulation site for a total of 320 trials. Trial order was counterbalanced such that the full design (combination of cue type, target type, and validity) was presented in each chunk of 20 trials. To familiarise participants with the task requirements, they first performed 48 practice trials where the verbal cue was replaced with an "x". Stimulation site was blocked, with initial site alternated across participants (11 participants started with EBA stimulation and 10 with OPA stimulation in both tasks). Participants were invited to take a short break every 32 trials.

QUANTIFICATION AND STATISTICAL ANALYSIS

Data pre-processing and analyses were conducted using R (Version 3.5.1) [57] packages: “dplyr” (pre-processing) [58] and “ez” (ANOVAs) [59]. Effect sizes were calculated using Jamovi (Version 0.9) [60]. Figures were generated using R package “ggplot2” [61].

Analysis

Statistical significance was tested with factorial design ANOVAs and follow-up t-tests. Significance level was set at $p = 0.05$. In accord with our instructions to participants to respond quickly and accurately, we report analyses of efficiency, computed for each condition and participant as the mean of accurate response times divided by the proportion correct. This measure assesses the effects of stimulation and validity on speed and accuracy in the aggregate. Similar, albeit sometimes weaker, patterns of results were found in analyses of the mean accurate response times and of proportion correct: Site x Task x Validity mixed-design ANOVA on accurate response times, $F(1, 40) = 2.11$, $p=0.15$; on proportion correct, $F(1,40) = 5.83$, $p=0.02$. Descriptive statistics for all measures (efficiency, accurate response time, and proportion correct) are detailed in Table S2.

DATA AND CODE AVAILABILITY

The datasets generated during this study are available at the Open Science Framework Repository: https://osf.io/cysw3/

REFERENCES

1. Bruner, J. S. and Postman, L. (1949). On the perception of incongruity: A paradigm. J. Personality *18*, 206-223.
2. de Lange, F. P., Heilbron, M. and Kok, P. (2018). How do expectations shape perception? Trends Cogn. Sci. *22*, 764-779.
3. Lupyan, G. and Clark, A. (2015). Words and the world: Predictive coding and the language-perception-cognition interface. Curr. Direct. Psychol. Sci. *24*, 279-284.
4. Summerfield, C. and Egner, T. (2009). Expectation (and attention) in visual cognition. Trends Cogn. Sci. *13*, 403-409.
5. Battistoni, E., Stein, T. and Peelen, M. V. (2017). Preparatory attention in visual cortex. Ann. N. Y. Acad. Sci. *1396*, 92-107.
6. Carrasco, M. (2011). Visual attention: the past 25 years. Vision Res. *51*, 1484-1525.
7. Simanova, I., Francken, J. C., de Lange, F. P. and Bekkering, H. (2016). Linguistic priors shape categorical perception. Lang. Cogn. Neurosci. *31*, 159-165.
8. Summerfield, C. and de Lange, F. P. (2014). Expectation in perceptual decision making: neural and computational mechanisms. Nat. Rev. Neurosci. *15*, 745-756.
9. Kok, P., Failing, M. F. and de Lange, F. P. (2014). Prior expectations evoke stimulus templates in the primary visual cortex. J. Cogn. Neurosci. *26*, 1546-1554.
10. Esterman, M. and Yantis, S. (2010). Perceptual expectation evokes category-selective cortical activity. Cereb. Cortex *20*, 1245-1253.
11. Puri, A. M., Wojciulik, E. and Ranganath, C. (2009). Category expectation modulates baseline and stimulus-evoked activity in human inferotemporal cortex. Brain Res. *1301*, 89-99.
12. Kok, P., Mostert, P. and de Lange, F. P. (2017). Prior expectations induce prestimulus sensory templates. Proc. Natl. Acad. Sci. U. S. A. *114*, 10473-10478.
13. Peelen, M. V. and Kastner, S. (2011). A neural basis for real-world visual search in human occipitotemporal cortex. Proc. Natl. Acad. Sci. U. S. A. *108*, 12125-12130.
14. Stokes, M., Thompson, R., Nobre, A. C. and Duncan, J. (2009). Shape-specific preparatory activity mediates attention to targets in human visual cortex. Proc. Natl. Acad. Sci. U. S. A. *106*, 19569-19574.
15. Johnstone, L. T. and Downing, P. E. (2017). Dissecting the visual perception of body shape with the Garner selective attention paradigm. Vis. Cogn. *25*, 507-523.
16. Lupyan, G. and Thompson-Schill, S. L. (2012). The evocative power of words: activation of concepts by verbal and nonverbal means. J. Exp. Psychol. Gen. *141*, 170-186.
17. Downing, P. E. and Peelen, M. V. (2011). The role of occipitotemporal body-selective regions in person perception. Cogn. Neurosci. *2*, 186-203.
18. Zimmermann, M., Verhagen, L., de Lange, F. P. and Toni, I. (2016). The extrastriate body area computes desired goal states during action planning. eNeuro *3*, e0020-16.2016 1-13.
19. Dillon, M. R., Persichetti, A. S., Spelke, E. S. and Dilks, D. D. (2018). Places in the brain: Bridging layout and object geometry in scene-selective cortex. Cereb. Cortex *28*, 2365-2374.
20. Julian, J. B., Ryan, J., Hamilton, R. H. and Epstein, R. A. (2016). The occipital place area is causally involved in representing environmental boundaries during navigation. Curr. Biol. *26*, 1104-1109.

21. Dilks, D. D., Julian, J. B., Paunov, A. M. and Kanwisher, N. (2013). The occipital place area is causally and selectively involved in scene perception. J. Neurosci. *33*, 1331-1336.
22. Downing, P. E. and Peelen, M. V. (2016). Body selectivity in occipitotemporal cortex: Causal evidence. Neuropsychologia *83*, 138-148.
23. Pitcher, D., Charles, L., Devlin, J. T., Walsh, V. and Duchaine, B. (2009). Triple dissociation of faces, bodies, and objects in extrastriate cortex. Curr. Biol. *19*, 319-324.
24. Pitcher, D., Goldhaber, T., Duchaine, B., Walsh, V. and Kanwisher, N. (2012). Two critical and functionally distinct stages of face and body perception. J. Neurosci. *32*, 15877-15885.
25. Urgesi, C., Berlucchi, G. and Aglioti, S. M. (2004). Magnetic stimulation of extrastriate body area impairs visual processing of nonfacial body parts. Curr. Biol. *14*, 2130-2134.
26. van Koningsbruggen, M. G., Peelen, M. V. and Downing, P. E. (2013). A causal role for the extrastriate body area in detecting people in real-world scenes. J. Neurosci. *33*, 7003-7010.
27. Hock, A., Kangas, A., Zieber, N. and Bhatt, R. S. (2015). The development of sex category representation in infancy: matching of faces and bodies. Dev. Psychol. *51*, 346-352.
28. Johnson, K. L. and Tassinary, L. G. (2005). Perceiving sex directly and indirectly: meaning in motion and morphology. Psychol. Sci. *16*, 890-897.
29. Hill, M. Q., Streuber, S., Hahn, C. A., Black, M. J. and O'Toole, A. J. (2016). Creating Body Shapes From Verbal Descriptions by Linking Similarity Spaces. Psychol. Sci. *27*, 1486-1497.
30. Chun, M. M., Golomb, J. D. and Turk-Browne, N. B. (2011). A taxonomy of external and internal attention. Ann. Rev. Psychol. *62*, 73-101.
31. Kok, P., Jehee, J. F. and de Lange, F. P. (2012). Less is more: expectation sharpens representations in the primary visual cortex. Neuron *75*, 265-270.
32. Yon, D., Gilbert, S. J., de Lange, F. P. and Press, C. (2018). Action sharpens sensory representations of expected outcomes. Nat. Commun. *9*, 4288.
33. Greene, M. R. (2013). Statistics of high-level scene context. Front. Psychol. *4*, 777.
34. Malcolm, G. L., Groen, I. I. A. and Baker, C. I. (2016). Making sense of real-world scenes. Trends. Cogn. Sci. *20*, 843-856.
35. Biederman, I., Mezzanotte, R. J. and Rabinowitz, J. C. (1982). Scene perception: Detecting and judging objects undergoing relational violations. Cogn. Psychol. *14*, 143-177.
36. Davenport, J. L. and Potter, M. C. (2004). Scene consistency in object and background perception. Psychol. Sci. *15*, 559-564.
37. Peelen, M. V. and Kastner, S. (2014). Attention in the real world: toward understanding its neural basis. Trends Cogn. Sci. *18*, 242-250.
38. Oliva, A. and Torralba, A. (2001). Modeling the shape of the scene: A holistic representation of the spatial envelope. International J. Computer Vision *42*, 145-175.
39. Kamps, F. S., Julian, J. B., Kubilius, J., Kanwisher, N. and Dilks, D. D. (2016). The occipital place area represents the local elements of scenes. Neuroimage *132*, 417-424.
40. Troiani, V., Stigliani, A., Smith, M. E. and Epstein, R. A. (2014). Multiple object properties drive scene-selective regions. Cereb. Cortex *24*, 883-897.
41. Meteyard, L. and Holmes, N. P. (2018). TMS SMART - Scalp mapping of annoyance ratings and twitches caused by Transcranial Magnetic Stimulation. J. Neurosci. Methods *299*, 34-44.
42. Henriksson, L., Mur, M. and Kriegeskorte, N. (2019). Rapid invariant encoding of scene layout in human OPA. Neuron doi:10.1016/j.neuron.2019.04.014.

43. Panichello, M. F., Cheung, O. S. and Bar, M. (2012). Predictive feedback and conscious visual experience. Front. Psychol. *3*, 620.
44. Summerfield, C. et al. (2006). Predictive codes for forthcoming perception in the frontal cortex. Science *314*, 1311-1314.
45. Ambrus, G. G., Amado, C., Krohn, L. and Kovács, G. (2019). TMS of the occipital face area modulates cross-domain identity priming. Brain Struct. Funct. *224*, 149-157.
46. Bergmann, T. O. (2018). Brain State-Dependent Brain Stimulation. Front. Psychol. *9*, 2108.
47. Silvanto, J., Muggleton, N. and Walsh, V. (2008). State-dependency in brain stimulation studies of perception and cognition. Trends Cogn. Sci. *12*, 447-454.
48. Ralph, M. A. L., Jefferies, E., Patterson, K. and Rogers, T. T. (2017). The neural and computational bases of semantic cognition. Nat. Rev. Neurosci. *18*, 42-55.
49. Rossi, S., Hallett, M., Rossini, P. M. and Pascual-Leone, A. (2009). Safety, ethical considerations, and application guidelines for the use of transcranial magnetic stimulation in clinical practice and research. Clin. Neurophys. *120*, 2008-2039.
50. Rossi, S., Hallett, M., Rossini, P. M. and Pascual-Leone, A. (2011). Screening questionnaire before TMS: an update. Clin. Neurophys. *122*, 1686.
51. Wellcome Centre for Human Neuroimaging (2014) SPM12 Statistical Parametric Mapping software. www.fil.ion.ucl.ac.uk/spm/software/spm12/
52. Rossini, P. M. et al. (2015). Non-invasive electrical and magnetic stimulation of the brain, spinal cord, roots and peripheral nerves: basic principles and procedures for routine clinical and research application. An updated report from an IFCN Committee. Clin. Neurophys. *126*, 1071-1107.
53. Urgesi, C., Candidi, M., Ionta, S. and Aglioti, S. M. (2007). Representation of body identity and body actions in extrastriate body area and ventral premotor cortex. Nat. Neurosci. *10*, 30-31.
54. Urgesi, C., Calvo-Merino, B., Haggard, P. and Aglioti, S. M. (2007). Transcranial magnetic stimulation reveals two cortical pathways for visual body processing. J. Neurosci. *27*, 8023-8030.
55. Brainard, D. H. and Vision, S. (1997). The psychophysics toolbox. Spatial Vis. *10*, 433-436.
56. Eaton, J. W., Bateman, D., Hauberg, S. and Wehbring, R. (2018). GNU Octave version 4.4.1 manual. https://octave.org/doc/v4.4.1/
57. R Core Team. (2019). R: A language and environment for statistical computing. R Foundation for Statistical Computing, Vienna, Austria.
58. Wickham, H., François, R., L. H. and, K. M. (2019). dplyr: A Grammar of Data Manipulation. R package version 0.8.0.1. https://dplyr.tidyverse.org/
59. Lawrence, M. A. (2016). ez: Easy Analysis and Visualization of Factorial Experiments. R package version 4.4-0. https://rdrr.io/cran/ez/
60. Jamovi project. (2019). jamovi (Version 0.9). https://www.jamovi.org/
61. Wickham, H. (2016). ggplot2: elegant graphics for data analysis (New York: Springer).

KEY RESOURCES TABLE

REAGENT or RESOURCE	SOURCE	IDENTIFIER
Deposited Data		
Raw data	This paper	https://osf.io/cysw3/
Software and Algorithms		
Octave (version 4.4)	[56]	https://www.gnu.org/software/octave/
Psychtoolbox (version 3.0.14)	[55]	http://psychtoolbox.org/
R (version 3.5.1)	[57]	https://www.R-project.org/
Jamovi (version 0.9)	[60]	https://www.jamovi.org
ggplot 2	[61]	https://ggplot2.tidyverse.org/
Dplyr (version 0.8.1)	[58]	https://CRAN.R-project.org/package=dplyr
Ez (version 4.4)	[59]	https://CRAN.R-project.org/package=ez
Brainsight (version 2.3.10)	Rogue-Research Inc.	https://www.rogue-research.com/
Matlab (version r2015b)	The Mathworks Inc.	https://mathworks.com/products/matlab.html
SPM (version 12)	[51]	www.fil.ion.ucl.ac.uk/spm/software/spm12/

Figure 1

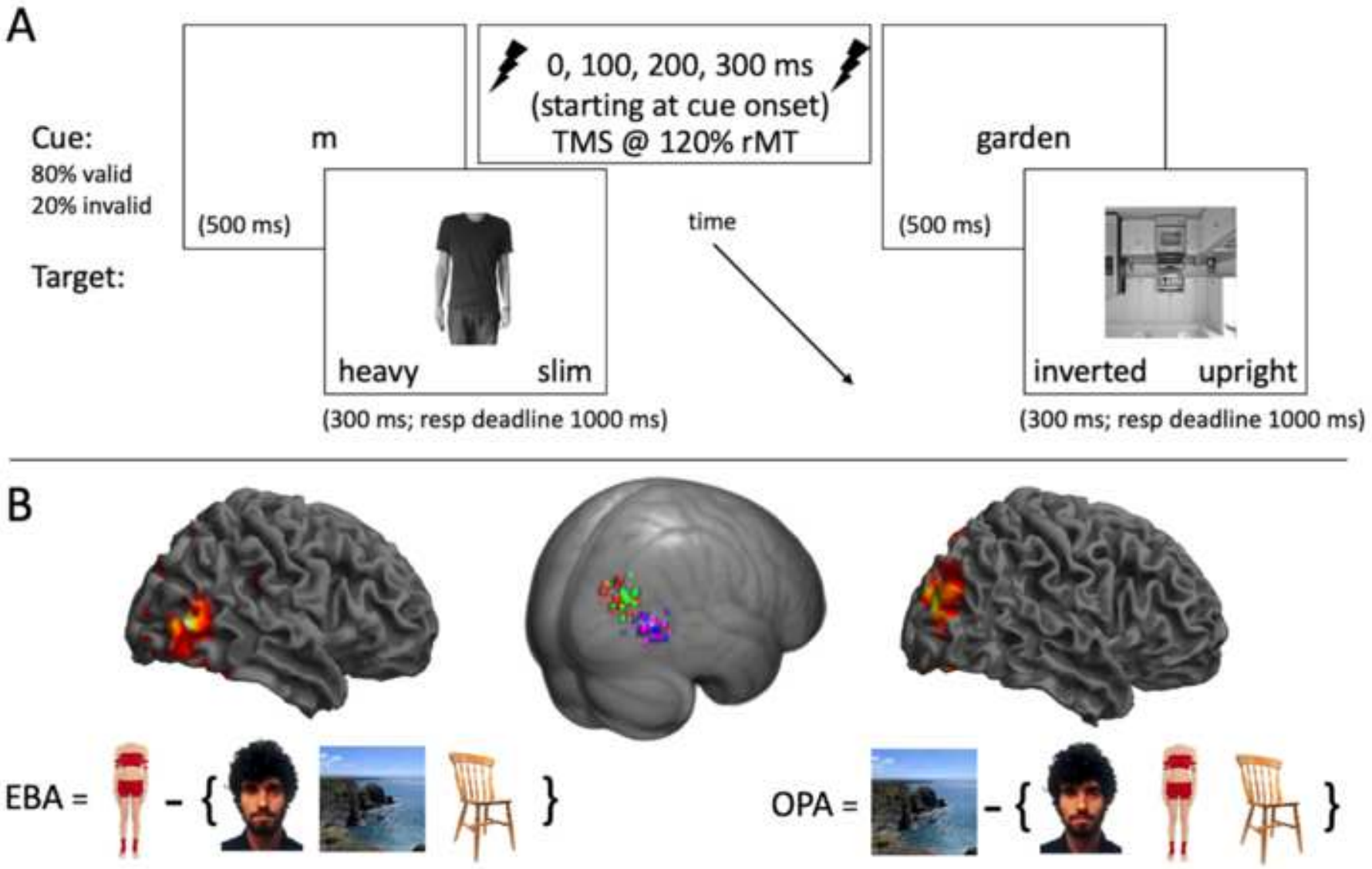

Figure 2

Click here to access/download;Figure;Figure 2.tiff

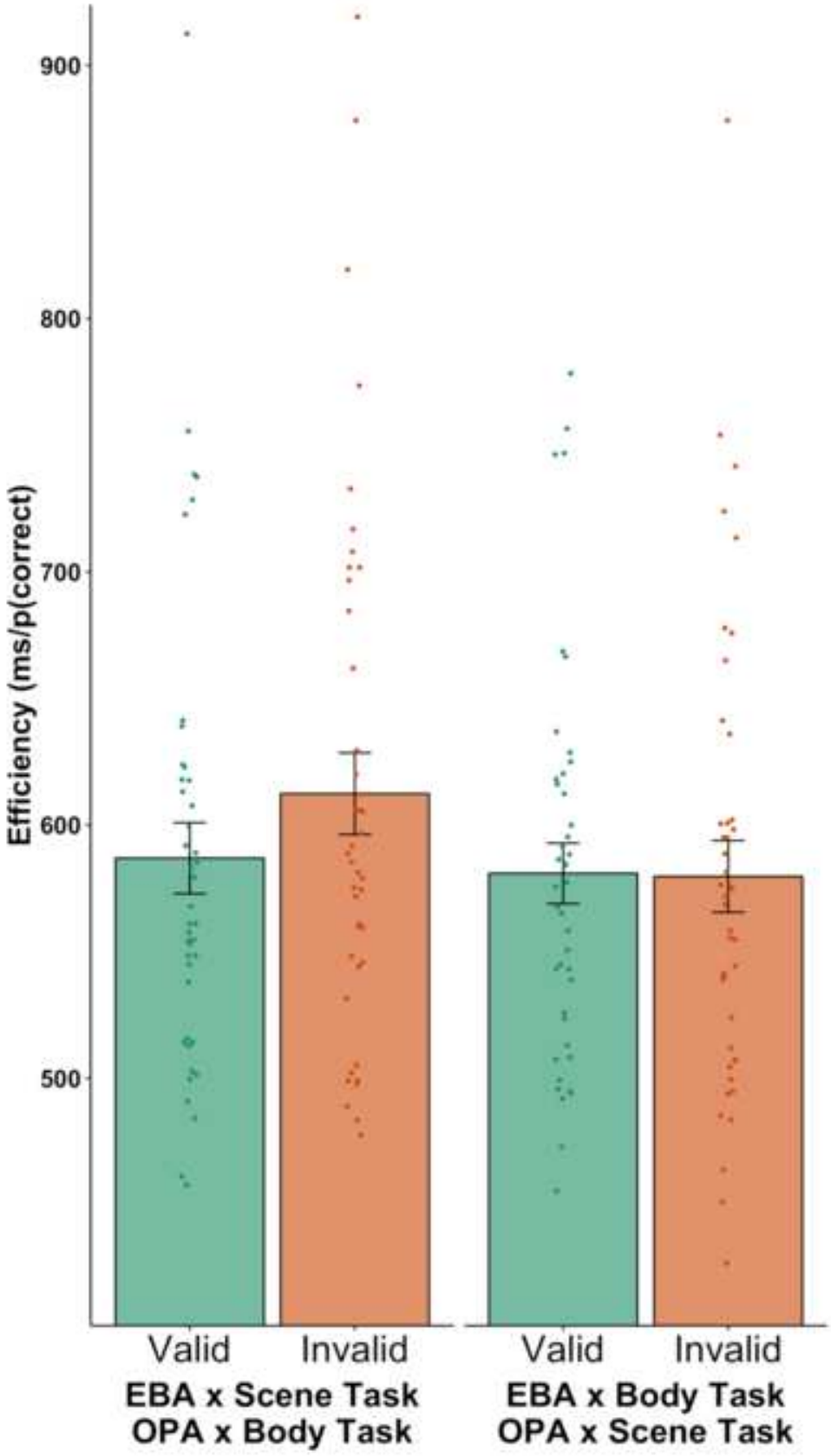

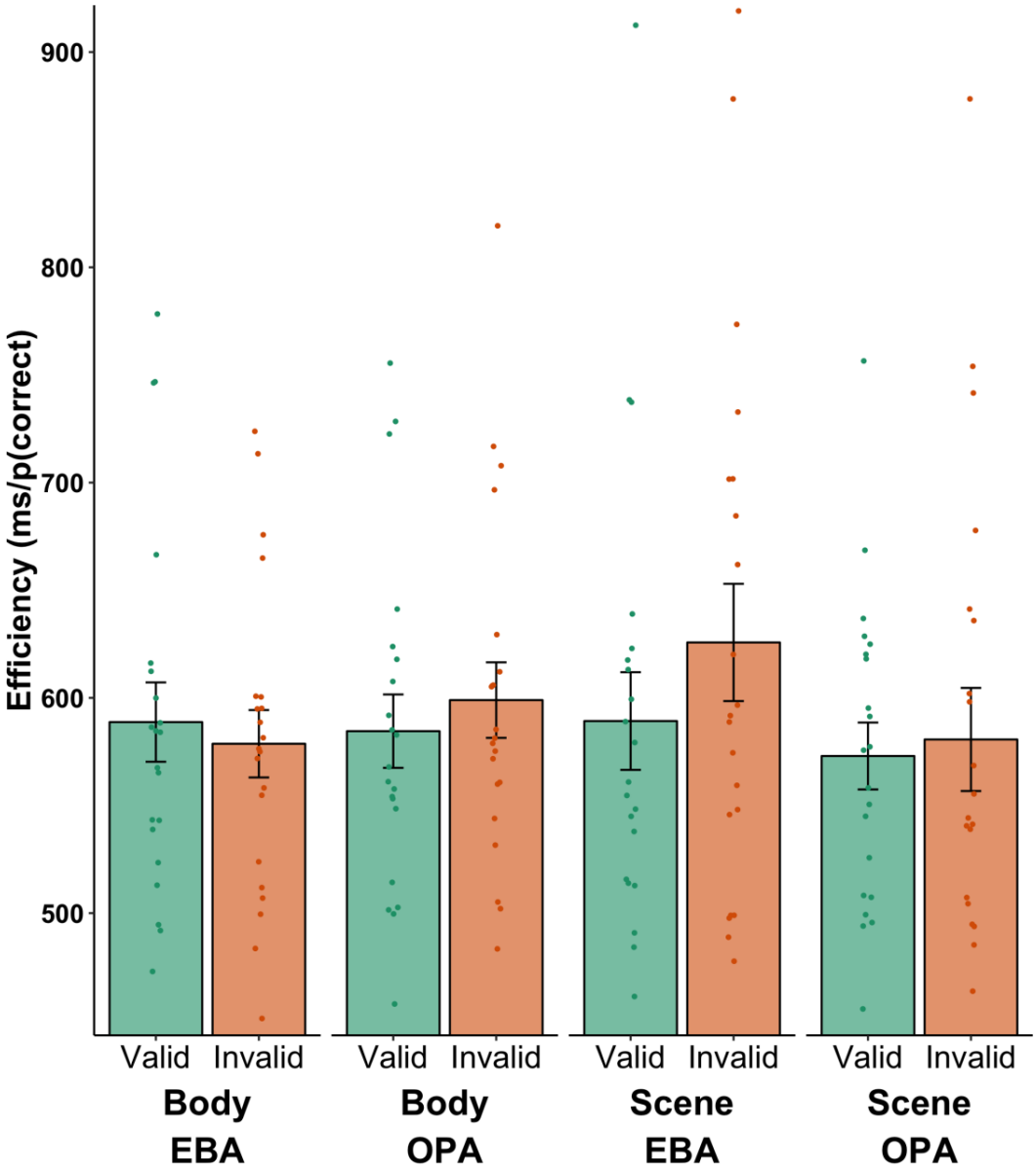

Figure S1. Impact of TMS over extrastriate category-selective regions on cue-driven stimulus expectations, related to Figure 2. Mean efficiency scores across participants (RT / p(correct)) are plotted in relation to cue validity, task, and stimulation site. Bars indicate mean values; error bars SE of the mean (including within- and between-participants variance); individual points reflect scores for each participant.

ID	Task	Area	x	y	z
1-1	Body	EBA	40.00	-73.00	-2.00
1-2	Body	EBA	48.00	-65.00	0.00
1-3	Body	EBA	51.00	-70.00	9.00
1-4	Body	EBA	46.00	-74.00	11.00
1-5	Body	EBA	50.00	-65.00	6.00
1-6	Body	EBA	52.00	-65.00	-1.00
1-7	Body	EBA	52.00	-59.00	-1.00
1-8	Body	EBA	48.00	-72.00	-2.00
1-9	Body	EBA	45.00	-59.00	3.00
1-10	Body	EBA	50.00	-69.00	-1.00
1-11	Body	EBA	44.00	-74.00	6.00
1-12	Body	EBA	44.00	-71.00	10.00
1-13	Body	EBA	49.00	-73.00	3.00
1-14	Body	EBA	40.00	-70.00	0.00
1-15	Body	EBA	51.00	-78.00	3.00
1-16	Body	EBA	53.00	-70.00	-2.00
1-17	Body	EBA	49.00	-76.00	-5.00
1-18	Body	EBA	50.00	-67.00	1.00
1-19	Body	EBA	43.00	-80.00	2.00
1-20	Body	EBA	44.00	-70.00	2.00
1-21	Body	EBA	52.00	-65.00	1.00
2-1	Scene	EBA	50.00	-68.00	1.00
2-2	Scene	EBA	44.00	-64.00	5.00
2-3	Scene	EBA	45.00	-80.00	-2.00
2-4	Scene	EBA	45.00	-76.00	-1.00
2-5	Scene	EBA	52.00	-70.00	-1.00
2-6	Scene	EBA	41.00	-80.00	16.00
2-7	Scene	EBA	47.00	-54.00	2.00
2-8	Scene	EBA	43.00	-81.00	-1.00
2-9	Scene	EBA	43.00	-76.00	6.00
2-10	Scene	EBA	47.00	-73.00	-7.00
2-11	Scene	EBA	46.00	-76.00	-2.00

2-12	Scene	EBA	56.00	-58.00	-8.00
2-13	Scene	EBA	50.00	-69.00	-3.00
2-14	Scene	EBA	57.00	-73.00	2.00
2-15	Scene	EBA	49.00	-75.00	3.00
2-16	Scene	EBA	55.00	-71.00	1.00
2-17	Scene	EBA	55.00	-79.00	5.00
2-18	Scene	EBA	46.00	-78.00	7.00
2-19	Scene	EBA	49.00	-70.00	2.00
2-20	Scene	EBA	51.00	-77.00	3.00
2-21	Scene	EBA	49.00	-70.00	1.00
1-1	Body	OPA	36.00	-83.00	15.00
1-2	Body	OPA	26.00	-75.00	23.00
1-3	Body	OPA	31.00	-71.00	16.00
1-4	Body	OPA	33.00	-75.00	34.00
1-5	Body	OPA	35.00	-76.00	8.00
1-6	Body	OPA	38.00	-73.00	25.00
1-7	Body	OPA	30.00	-78.00	7.00
1-8	Body	OPA	29.00	-77.00	21.00
1-9	Body	OPA	37.00	-75.00	23.00
1-10	Body	OPA	29.00	-78.00	25.00
1-11	Body	OPA	23.00	-83.00	28.00
1-12	Body	OPA	32.00	-77.00	15.00
1-13	Body	OPA	40.00	-76.00	17.00
1-14	Body	OPA	25.00	-81.00	15.00
1-15	Body	OPA	29.00	-76.00	20.00
1-16	Body	OPA	36.00	-77.00	20.00
1-17	Body	OPA	35.00	-80.00	23.00
1-18	Body	OPA	38.00	-73.00	24.00
1-19	Body	OPA	40.00	-83.00	21.00
1-20	Body	OPA	37.00	-76.00	18.00
1-21	Body	OPA	35.00	-80.00	20.00
2-1	Scene	OPA	32.00	-75.00	23.00
2-2	Scene	OPA	30.00	-81.00	15.00
2-3	Scene	OPA	36.00	-84.00	15.00
2-4	Scene	OPA	26.00	-79.00	23.00

2-5	Scene	OPA	31.00	-78.00	9.00
2-6	Scene	OPA	24.00	-82.00	30.00
2-7	Scene	OPA	45.00	-71.00	25.00
2-8	Scene	OPA	35.00	-86.00	24.00
2-9	Scene	OPA	29.00	-81.00	18.00
2-10	Scene	OPA	35.00	-72.00	5.00
2-11	Scene	OPA	33.00	-78.00	19.00
2-12	Scene	OPA	35.00	-79.00	17.00
2-13	Scene	OPA	37.00	-79.00	15.00
2-14	Scene	OPA	46.00	-85.00	15.00
2-15	Scene	OPA	37.00	-87.00	18.00
2-16	Scene	OPA	42.00	-82.00	25.00
2-17	Scene	OPA	34.00	-90.00	26.00
2-18	Scene	OPA	36.00	-86.00	24.00
2-19	Scene	OPA	34.00	-83.00	20.00
2-20	Scene	OPA	38.00	-86.00	15.00
2-21	Scene	OPA	30.00	-81.00	21.00

Table S1. MNI coordinates of peak locations identified in independent functional localizers and targeted for TMS, related to Figure 1. Separate groups of participants performed each task.

Accuracy (Proportion Correct)			
Condition	*M*	*M* 95% CI [LL, UL]	*SD*
Body-EBA-Valid	0.89	[0.86, 0.92]	0.07
Body-EBA-Invalid	0.91	[0.88, 0.94]	0.07
Body-OPA-Valid	0.91	[0.89, 0.94]	0.06
Body-OPA-Invalid	0.92	[0.89, 0.94]	0.06
Scene-EBA-Valid	0.90	[0.87, 0.93]	0.06
Scene-EBA-Invalid	0.87	[0.83, 0.91]	0.09
Scene-OPA-Valid	0.90	[0.87, 0.93]	0.07
Scene-OPA-Invalid	0.91	[0.87, 0.94]	0.08
Response Times in ms			
Condition	*M*	*M* 95% CI [LL, UL]	*SD*
Body-EBA-Valid	523.64	[483.07, 564.21]	89.13
Body-EBA-Invalid	528.91	[489.37, 568.46]	86.88
Body-OPA-Valid	534.07	[497.21, 570.94]	80.98
Body-OPA-Invalid	549.09	[509.24, 588.95]	87.56
Scene-EBA-Valid	525.21	[491.73, 558.70]	73.56
Scene-EBA-Invalid	537.98	[501.82, 574.14]	79.44
Scene-OPA-Valid	514.87	[483.97, 545.76]	67.87
Scene-OPA-Invalid	522.44	[482.62, 562.26]	87.48
Efficiency (Response Times in ms / Proportion Correct)			
Condition	*M*	*M* 95% CI [LL, UL]	*SD*

Body-EBA-Valid	588.76	[550.33, 627.19]	84.43
Body-EBA-Invalid	578.68	[546.03, 611.34]	71.74
Body-OPA-Valid	584.54	[548.99, 620.10]	78.10
Body-OPA-Invalid	598.97	[562.36, 635.57]	80.42
Scene-EBA-Valid	589.24	[541.93, 636.56]	103.95
Scene-EBA-Invalid	625.75	[568.94, 682.55]	124.79
Scene-OPA-Valid	573.00	[540.57, 605.43]	71.24
Scene-OPA-Invalid	580.68	[530.71, 630.64]	109.76

Table S2. Means and standard deviations for accuracy, response times, and efficiency in each condition, related to Figure 2. Naming convention: Task-Stimulation Site-Condition; e.g. Body-EBA-Valid describes performance on valid trials from the body task under stimulation over extrastriate body area (EBA). M and SD represent mean and standard deviation, respectively. LL and UL indicate the lower and upper limits of the 95% confidence interval for the mean, respectively.